Separation and Purification Technology 147 (2015) 303–310

Contents lists available at ScienceDirect

Separation and Purification Technology

journal homepage: www.elsevier.com/locate/seppur

Hydraulically irreversible fouling on ceramic MF/UF membranes: Comparison of fouling indices, foulant composition and irreversible pore narrowing

Ran Shang [a,*], Francois Vuong [a], Jingyi Hu [a], Sheng Li [a,b], Antoine J.B. Kemperman [c], Kitty Nijmeijer [c], Emile R. Cornelissen [d], Sebastiaan G.J. Heijman [a], Luuk C. Rietveld [a]

[a] Department of Sanitary Engineering, Faculty of Civil Engineering and Geosciences, Delft University of Technology, P.O. Box 5048, 2600 GA Delft, The Netherlands
[b] Water Desalination and Reuse Research Center, 4700 King Abdullah University of Science and Technology, Thuwal 23955-6900, Saudi Arabia
[c] Membrane Science and Technology, MESA+ Institute for Nanotechnology, Faculty of Science and Technology, University of Twente, P.O. Box 217, NL-7500 AE Enschede, The Netherlands
[d] KWR Watercycle Research Institute, P.O. Box 1072, 3430 BB Nieuwegein, The Netherlands

ARTICLE INFO

Article history:
Received 25 February 2015
Received in revised form 27 April 2015
Accepted 28 April 2015
Available online 7 May 2015

Keywords:
Ceramic membrane
Natural organic matter
Pore size distribution
LC-OCD
Hydraulically irreversible fouling

ABSTRACT

The application of ceramic membranes in water treatment is becoming increasing attractive because of their long life time and excellent chemical, mechanical and thermal stability. However, fouling of ceramic membranes, especially hydraulically irreversible fouling, is still a critical aspect affecting the operational cost and energy consumption in water treatment plants. In this study, four ceramic membranes with pore sizes or molecular weight cut-off (MWCO) of 0.20 μm, 0.14 μm, 300 kDa and 50 kDa were compared during natural surface water filtration with respect to hydraulically irreversible fouling index (HIFI), foulant composition and narrowing of pore size due to the irreversible fouling. Our results showed that the hydraulically irreversible fouling index (HIFI) was proportional to the membrane pore size ($r^2 = 0.89$) when the same feed water was filtrated. The UF membranes showed lower HIFI values than the MF membranes. Pore narrowing (internal fouling) was found to be a main fouling pattern of the hydraulically irreversible fouling. The internal fouling was caused by monolayer adsorption of foulants with different sizes that is dependent on the size of the membrane pore.

© 2015 Elsevier B.V. All rights reserved.

1. Introduction

In recent years, growing interest in the application of ceramic membranes in water treatment has emerged, due to their longer operational life and higher chemical, mechanical and thermal stability as compared to polymeric membranes [1,2]. Although the capital costs of ceramic membranes are still higher than polymeric membranes, new technologies have been investigated to reduce the investment costs of the ceramic membrane systems, such as CeraMac®, a system housing up to 200 ceramic membrane modules in a single stainless steel vessel [3]. Ceramic membranes can be made to have fairly uniform pores in size, but defects, if occur in the ceramic membranes, will ruin the permeate water quality [4]. It is also reported that ceramic membranes offer a better permeate water quality and exhibit a lower trans-membrane pressure (TMP) increase than polymeric membranes due to their higher porosity and more uniform pores [5,6]. However, fouling on ceramic membranes, especially the hydraulically irreversible fouling, can still be severe, with consequences for increased operational costs and energy consumption.

Ceramic membranes exhibit different fouling behaviors compared to polymeric membranes. Mueller et al. [7] observed less hydraulically irreversible fouling on a TiO_2 membrane with Al_2O_3 support than on a polyethersulfone (PES) polymeric membrane during surface water filtration, probably due to less biopolymer fouling on the TiO_2 membrane as determined by liquid chromatography with an organic carbon detector (LC-OCD). Hofs et al. [6] also reported less hydraulically irreversible fouling on ceramic membranes in comparison with a polymeric one, and they attribute this to a higher volume/area ratio on the tested ceramic membranes modules resulting in different hydraulic conditions. When filtrating algae organic matter (AOM) released from *Microcystis aeruginosa*, a dominant cyanobacterium in reservoirs or lakes during seasonal algae bloom, the hydrophilic fractions in AOM contribute to the hydraulically irreversible fouling on a ceramic membrane

* Corresponding author. Tel.: +31 15 2783539.
E-mail addresses: r.shang@tudelft.nl, r.shang@outlook.com (R. Shang).

http://dx.doi.org/10.1016/j.seppur.2015.04.039
1383-5866/© 2015 Elsevier B.V. All rights reserved.

(ZrO_2–TiO_2) [8], while the hydrophobic fractions were mainly found in the irreversible fouling layer of a polymeric membrane (PES) [9].

Natural surface waters contain a matrix of organic matter and particles in both the nanometer or micrometer range. Humic substances [10–14] and biopolymers [15–21] in natural surface water have been intensively acknowledged as the main organic foulants on UF/MF membranes in both hydraulically reversible and irreversible fouling. Zheng et al. [22] identified organic matter larger than the UF pore size as the major foulants, which contribute to the cake layer formation, while only a small remaining portion (unquantified) remains as hydraulically irreversible fouling after backwash. Zhang et al. [23] reported that high molecular weight biopolymers greatly contribute to the flux deterioration. Tian et al. and Kimura et al. observed correlation between biopolymers and the fouling in both UF [20] and MF [21] membranes. Moreover, Howe and Clark [24] found that the organic matter and particles in natural water ranging from 3 nm to 14 nm in size predominately contribute to the fouling of MF and UF membranes. The inorganic particles in the nanometer and micrometer range, existing in natural surface water, also exacerbate the membrane fouling by hindering the back diffusion of organic matter from the membrane surface [25,26].

The membrane fouling pattern is different for membranes with different pore sizes, while only a few studies treated this aspect. Jin et al. [27] observed that, in a membrane bioreactor (MBR) system, the membrane pore size plays a more important role in the fouling potential than the organic composition, molecular weight distribution and zeta potential of the feed water. Mafirad et al. [28] found that the irreversible fouling was less on membrane with smaller pore size in an MBR system for oily wastewater treatment. Similarly, membrane fouling caused by surface water or secondary effluent water is also influenced by the membrane pore size, which was reported in several studies [24,29–31]. However, the effect of the pore size on hydraulically irreversible fouling during natural surface water filtration has not been yet systematically studied.

In this paper, the hydraulically irreversible fouling of four UF and MF ceramic membranes was systematically investigated upon constant flux filtration of a natural surface water. Organic matter in the feed water and on the membrane surface was characterized by LC-OCD to quantitatively elucidate the main organic fractions that lead to irreversible fouling on the membranes with various pore sizes. Permeate water from every tested membrane was reutilized as feed to study the adsorptive fouling (internal fouling) and its irreversibility on membrane fouling.

2. Materials and methods

2.1. Filtration setup and the fouling experiment protocol

The filtration setup (Fig. 1) was designed for constant flux filtration experiments with a constant flux backwash option. The constant feed and backwash flow were driven by two pairs of programmable DUAL syringe pumps (New Era Pump Systems, Inc.). The DUAL syringe pump system has a continuous infusion mode, allowing one syringe pump to infuse when the other withdraws. Two solenoid valves (Bürkert) were applied to control the direction of the water flow. The syringe pumps and solenoid valves were controlled by a programmable logic controller. Two digital pressure meters were used to measure the pressure during filtration feed flow and backwash feed flow. Since the pressure of the permeate water and the backwash waste stream side was equal to atmospheric pressure, the pressure on these two pressure meters was the trans-membrane pressure (TMP), which was logged to a computer every 8 s.

Three operational phases were employed for this setup: filtration (production), forward flush (from feed vessel to backwash-waste vessel) and backwash.

The fouling experiments were composed of 12 cycles of the three operational phases in the following order: forward flush (9.4 m h^{-1} for 1.5 min), filtration (60 L m^{-2} h^{-1} for 15 min) and backwash with permeate water (120 L m^{-2} h^{-1} for 3 min). The purpose of using a forward flush is to purge the membrane module to remove the air or the backwash remaining liquid, and thus, a high crossflow velocity is not necessary. A moderate backwash flux of 120 L m^{-2} h^{-1} was chosen because the syringe pumps were not designed to drive high flows and high pressures. It needs to be noted that a different backwash condition may result in different hydraulic reversible and irreversible fouling.

Between different filtration runs, the membranes were chemically cleaned by soaking it in a sodium hypochlorite solution (1%) for at least 24 h to remove all the remaining organic foulants on the membranes. After the chemical cleaning, permeability of the ceramic membranes was completely restored and they could be used again for the next test. All the filtration cycles were carried out in dead-end filtration mode.

The feed water, permeate and backwash water from the first three cycles (cycles 1–3) and the last three cycles (cycles 8–12) were collected and used to determine the fractions in the bulk organic matter that were responsible for irreversible fouling. The first three cycles represent the fouling stage with interaction between the new membrane and foulant, while the last three cycles represent the interaction between the fouled membrane and the foulant. The collected samples were immediately pasteurized (in a water bath at 69 °C for 30 min) and stored in a refrigerator (4 °C) before further characterization, to prevent a change in the organic matter due to biodegradation.

2.2. Characterization of the surface water

Surface water was taken from the Schie Canal (Delft City, the Netherlands). The surface water was pre-treated by a 1 μm cartridge filter to remove coarse materials and most bacteria, and stored in a refrigerator (4 °C) as feed water for maximum 24 h. Before using it for the filtration experiments, the feed water was placed outside the refrigerator for several hours to reach room temperature (about 20 °C). The water quality parameters of the feed water are listed in Table 1.

2.3. Organic matter characterization by LC-OCD

LC-OCD was performed to fractionate the bulk organic matter in surface water into 5 categories according to Huber et al. [32]: biopolymers, humic substances, building blocks, low molecular-weight acids, and low molecular-weight neutrals. The calculated fraction that remains on the chromatography column is considered to be hydrophobic fraction of the organic carbon expressed as hydrophobic organic carbon (HOC). Due to the unknown error that exists in the calculation method of HOC [33], the HOC fraction is not used in this study. In the measured samples, the HOC fractions count for approximately 10% of the total dissolved NOM. The NOM fraction is mostly composed of biopolymers and humic substances. The biopolymers exhibit a molecular weight (MW) range of $\gg$20 kDa, and the humic substances are in a range of 0.45–1.15 kDa [32].

The hydraulic radius of organic matter was estimated using an empirical equation which holds for MW <100 kDa [34]:

$$r_h = 0.845 \cdot MW^{0.498} \quad (1)$$

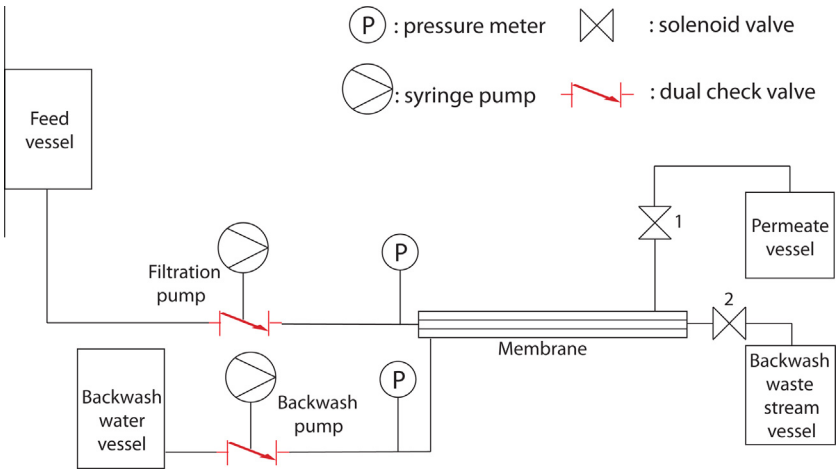

Fig. 1. Scheme of the filtration setup.

Table 1
Water quality of Schie Canal water[a].

Parameters	Values[b]	Parameters	Values[b]	Parameters	Values[b]	Parameters	Values[b]
pH	7.6 ± 0.2	Al	0.05 ± 0.02	K	12 ± 1	SO_4^{2-}	145 ± 6
DOC	12 ± 2	Fe	0.11 ± 0.09	Ba	0.01 ± 0.01	PO_4^{3-}	0.8 ± 0.3
Ca	117 ± 7	Mn	0.02 ± 0.10	Sr	0.45 ± 0.03		
Na	47 ± 3	Mg	19 ± 1	Cl	92 ± 5		

[a] Unit of each parameter is mg/l, except for pH.
[b] Average ± SD from triplicate measurements.

where r_h is the estimated hydraulic radius (nm); *MW* is the mean molecular weight (kDa).

According to Eq. (1), the hydraulic diameter of humic substances is estimated ranging from 1.1 to 1.8 nm, and the hydraulic diameter of biopolymers is >7.5 nm. The estimated values agree with those reported in the literature. Schimpf and Petteys [35] reported that the hydrodynamic diameter of humic substances is around 1.0 nm, measured by flow field flow fractionation. Fluorescence correlation spectroscopy gives a direct measurement of the values of diffusion coefficients, and the hydraulic diameter of humic substances is estimated to be 1.6–2.0 nm by Lead et al. [36]. It is reported that calculations using Stokes' law indicated the colloidal biopolymers in natural water are >10 nm [36,37].

All samples for the LC-OCD measurement were pasteurized (in a water bath at 69 °C for 30 min), filtered by a 0.45 μm filter and then sent via UPS express in an insulated shipping container with ice bags from Delft University of Technology in the Netherlands to King Abdullah University of Science and Technology in Saudi Arabia for LC-OCD analysis. After 2–3 days shipping, the samples were stored in a refrigerator at 4 °C until the measurements were conducted. Due to the high dissolved organic carbon (DOC) concentration, samples were diluted six times before the analysis. The effect of pasteurization on the chemical properties of the organic solutes is minor as recommended by the DOC-LABOR Dr. HUBER [38], manufacture of the LC-OCD analysis apparatus.

2.4. Ceramic UF and MF membranes

Commercial single channel tubular ceramic membranes with a MWCO or pore size of 50 kDa, 300 kDa, 0.14 μm and 0.20 μm were obtained from TAMI Industry (France). All the membranes consist of a TiO_2 support layer, with an operational temperature of 350 °C and a pH range of 0–14. The dimensions of the membranes are similar, with a length of 250 mm, outer diameter of 10 mm and an inner diameter of 6 mm. The membrane area of each module is 0.0047 m^2. More information as provided by the manufacturer is shown in Table 2.

2.5. Characterization and quantification of hydraulically irreversible fouling

The irreversible organic foulant is regarded as the organic components that remain after the hydraulic backwash, regardless that different organic components may lead to filtration resistance to different extents. It was calculated from the organic carbon mass balance. The organic composition that contributed to the total fouling ($TF_{LC\text{-}OCD}$), that was calculated from the LC-OCD results, was defined using Eq. (2):

$$TF_{LC-OCD} = (OC_{raw} - OC_{perm}) \times V_f \quad (2)$$

where $TF_{LC\text{-}OCD}$ is the total mass of organic foulants rejected by the membrane, expressed as the LC-OCD relative signal response multiplied by the volume (Rel. Signal Response × ml); OC_{raw} is expressed as the LC-OCD relative signal response of the feed water representing its organic fractions with their concentration (Rel. Signal Response); OC_{perm} is expressed as the LC-OCD relative signal

Table 2
Characteristics of the ceramic membranes.

	UF membranes		MF membranes	
MWCO/pore size	50 kDa/ 0.025 μm[a]	300 kDa/ 0.061 μm[a]	0.14 μm	0.20 μm
Active layer	ZrO_2	ZrO_2	TiO_2 & ZrO_2	TiO_2 & ZrO_2
Support	TiO_2	TiO_2	TiO_2	TiO_2
Specific flux (J_{S0}), L m^{-2} h^{-1} bar^{-1}	160	500	6450	6740

[a] The pore size of the UF membrane was calculated using Eq. (6).

response of the permeate water (Rel. Signal Response); V_f is the feed water volume (ml).

During the filtration, the permeate water was used for backwash, which contained certain organic matters (measured as OC_{perm}). The organic composition of the reversible foulants was derived from the difference of organic contents between the backwash water and the permeate water. Therefore, the organic composition of the hydraulically reversible foulants was quantified using Eq. (3):

$$HRF_{LC-OCD} = (OC_{bw} - OC_{perm}) \times V_{bw} \quad (3)$$

where $HRF_{LC\text{-}OCD}$ is the hydraulically reversible mass foulants on the membrane (Rel. Signal Response × ml); OC_{bw} is expressed as the LC-OCD relative signal response of the backwash water (Rel. Signal Response); and V_{bw} is the backwash water volume (ml).

The organic composition of the hydraulically irreversible fouling was thus determined using:

$$HIF_{LC-OCD} = TF_{LC-OCD} - HRF_{LC-OCD} \quad (4)$$

where $HIF_{LC\text{-}OCD}$ is the hydraulically irreversible mass foulants on the membrane (Rel. Signal Response × ml).

It is prudent to note that the calculated $HIF_{LC\text{-}OCD}$ is a relative HIF mass. The LC-OCD curves that were used for calculation show the dimensionless relative signal response, which, however, are strictly linearly correlated to organic concentration at certain elution time. Therefore, the relative HIF mass is represented by the relative signal response multiply by the volumes indicated above in the same section.

By using the syringe pumps and the programmable logic controller in the filtration setup that is described in Section 2.1, the volumes of backwash water and permeate water were known precisely. It ensures accurate mass calculations based on the concentrations and volumes.

2.6. Fouling experiment with permeate water

Internal fouling arises from the adsorption of organic matters that are smaller than the membrane pore size leading to the pore narrowing [16]. To determine internal fouling and its effect on hydraulically irreversible fouling, additional fouling experiments were carried out with the permeate water of the individual membranes. The permeate water was collected from each membrane after three cycles of filtration. Subsequently, the permeate water was filtrated again with the same membrane after it had been chemically cleaned. The filtration protocol and chemical cleaning procedure followed the fouling experiments protocol given in Section 2.1.

Particles that are larger than pore size were assumed not to be present in the permeate water, because the ceramic membranes are assumed to have a narrow pore size distribution. Although the largest pore sizes of the 0.20 μm and 0.14 μm MF membranes were measured as 0.6 and 1.0 μm, respectively, the majority (approximately 80%) of the pore sizes of the 0.20 μm and 0.14 μm MF membranes were narrowly distributed in the range of 0.187–0.193 μm and 0.127–0.130 μm, respectively (Supplementary Data, Fig. S2). In addition, minor defects were detected in the 50 kDa UF membrane according to its molecular weight cut-off measurement (Supplementary Data, Fig. S4), which may allow a small fraction of larger molecular organic matters than their pore sizes to exist in their permeate water.

2.7. Calculation of membrane pore sizes

A strong simplified method for membrane pore size estimation is to calculate the molecular diameter of the dextran with a molecular weight equal to the MWCO of the membrane [42,43]. Although this simplified method is widely adopted, the method does not include the role of diffusion and steric exclusion in the separation process.

When considering the filtration mechanisms including diffusion and steric exclusion, the solute permeability ratio is believed to be primarily determined by the ratio of pore size to solute size [39]. Based on this theory, the Ferry–Faxen equation [39] is derived to estimate the mean pore radius of membranes:

$$(1-R) = \left(1-\frac{r_h}{r_p}\right)^2 \cdot \left(1 - 0.104\frac{r_h}{r_p} - 5.21\left(\frac{r_h}{r_p}\right)^2 + 4.19\left(\frac{r_h}{r_p}\right)^3 + 4.18\left(\frac{r_h}{r_p}\right)^4 - 3.04\left(\frac{r_h}{r_p}\right)^5\right) \quad (5)$$

where R is the retention of a standard dextran; r_h is the hydraulic radius of dextran (nm); r_p is the pore radius of UF membranes (nm). Combining Eq. (1) and Eq. (5), the pore radius of the UF membranes can be determined by obtaining 90 percentile retention of the dextran with a molecular weight equal to the MWCO of the membrane (in kDa) [40], as calculated by:

$$r_p = 2.10 \cdot r_h = 1.77 \cdot MWCO^{0.498} \quad (6)$$

When deriving the Eq. (5), it is assumed that the solute molecules are spherical and they are located along the center of the pore axis. The solution in the pore is assumed to be sufficiently dilute that each molecule crosses the membrane independently [39,41].

2.8. Calculation and measurement of pore narrowing due to internal fouling

Pore narrowing caused by internal fouling was indirectly determined from the fouling profile during the permeate water filtration as described above in Section 2.6. Because particles and organic matters that are smaller than the pore size are mainly present in the permeate water of individual membrane, the increase in filtration resistance during permeate water filtration was considered to be mainly due to pore narrowing rather than cake layer growth. The pore radius (r_p) evolution during the filtration can be calculated using the Hagen–Poiseuille equation [44–47]:

$$r_p = \left(\frac{8 \times 10^{-5} \cdot \eta \cdot L \cdot Q}{n \cdot \pi \cdot \Delta P}\right)^{1/4} \quad (7)$$

where L is the pore length (m); Q is the fluid flow ($m^3\ s^{-1}$); n is the number of pores; r_p is the hydrodynamic pore radius (m) and L/n is the fitting parameter based on the clean membrane.

To validate the calculated pore size narrowing, the pore size distributions of both the clean and fouled MF membranes were measured by capillary flow porometry (Porolux 1000, IBFT GmbH, Germany). Due to the limitation of the applied pressure during the capillary flow porometry, this instrument could not be applied to determine the pore size of the UF membranes, and thus only theoretical calculation values were employed. A wetting liquid, Porefil (Benelux Scientific B.V., The Netherlands), was pressed through the pores of the membranes, while the flow rate and feed pressure were recorded in time. The pore size distribution was automatically calculated based on the Young–Laplace equation:

$$D = \frac{4\sigma \cdot \cos\varphi \cdot SF}{P} \quad (8)$$

where D is the diameter of the membrane pore (m), P is the applied pressure (bar), σ is the surface tension of the liquid (N/m), φ is the contact angle of the liquid on the material surface, and SF is the shape factor.

2.9. Fouling resistance and the hydraulically irreversible fouling index

To compare the irreversible fouling of the ceramic membranes with various pore sizes, the fouling resistance and hydraulically irreversible fouling index (HIFI) were calculated.

The filtration resistance was calculated by:

$$R = \frac{\Delta P}{\eta \cdot J} = \frac{\Delta P_0 + \Delta P_f}{\eta \cdot J} \quad (9)$$

where R is the filtration resistance (m^{-1}); ΔP is the trans-membrane pressure ($N\ m^{-2}$); ΔP_0 is the trans-membrane pressure of the clean membrane; ΔP_f is the pressure difference due to fouling; η is the dynamic viscosity ($N\ s\ m^{-2}$), calculated by $497 \times 10^{-3}/(t + 42.5)^{1.5}$ [48]; J is the flux ($m^3\ m^{-2}\ s^{-1}$) and t is the feed water temperature (°C).

A model based on a resistance-in-series approach was used to determine the HIFI ($m^2\ L^{-1}$) as follows [49]:

$$\frac{1}{J_s'} = 1 + (HIFI) \cdot V \quad (10)$$

where J_s' is the normalized specific flux, defined as $\Delta P_0/\Delta P$, when the filtration is under constant flux and V is the specific volume (permeate volume/membrane area). This fouling index is not attributed to a specific mechanism so the model can be valid regardless of whether cake filtration, pore constriction, or a combination of fouling mechanisms is occurring. The derivation of the Eq. (10) is reported in the Ref. [49]. If the rate of increase in resistance is linearly proportional to V (i.e. a plot of $(1/J_s')$ versus (V) data is linear), the HIFI can be quantified using linear regression. However, the rate of resistance increase might be a non-linear function of V. In that case, the HIFI can be determined using a 2-point method; i.e., instead of using all performance data, the first and the last points can be used to determine the average rate of increase in resistance [49]. In this study, the 2-point method was used.

3. Results and discussion

3.1. Organic characterization of hydraulically irreversible foulants

The mass balance calculations based on the LC-OCD analysis quantitatively illustrate the organic irreversible foulants during the first three cycles and the last three cycles (Fig. 2). On each tested membrane, both biopolymers and humic substances were found in the hydraulically irreversible foulants. The humic substance fraction is also evidenced by its UV absorbance simultaneously measured by the UV detector in the LC-OCD apparatus (Supplementary Data, Fig. S1). A higher amount of humic substances was observed in the hydraulically irreversible foulants than biopolymers. This is consistent with the observation of Mueller et al. [7]. They noted that humic substances have higher propensity than biopolymers to foul the ceramic membranes, while the opposite trend was observed for polymeric membranes.

As compared to the first three cycles, less amount of humic substances and biopolymers were identified as irreversible foulant during the last three cycles using the mass balance method. This could be partially explained by the adsorptive fouling mechanism that is more apparent at the beginning of the filtration process indicated by the first three cycles [24,50]. Throughout the filtration process, less adsorption sites were available on the membrane [11,50,51]. Consequently, the accumulation of organic foulants on the membrane decreased over time. In addition, the backwash in later cycles may also remove a fraction of reversible foulants from the previous cycles. This may lead to decreased calculate amount of HIF in the last 3 cycles, as observed in Fig. 2.

3.2. Pore narrowing (internal fouling) as a mechanism for hydraulically irreversible fouling

The organic matter in surface water causes membrane fouling in different ways (internal fouling or cake layer formation), depending on the pore size of the membranes. In order to distinguish between the contributions of either internal pore fouling or cake layer formation on the fouling resistance during filtration, additional experiments were carried out. The fouling resistance during permeate water filtration represented the internal fouling resistance, with negligible cake layer resistance, since it was caused by foulants that were mainly smaller than the pore size (Supplementary Data, Fig. S3). The difference between the internal fouling resistance and the fouling resistance in surface water filtration represented the fouling resistance due to cake formation and pore blocking. It was found that during surface water filtration, the hydraulic backwash could partially decrease the fouling resistance, while the fouling resistance increase during the permeate water filtration could not be recovered by the hydraulic backwash of the membranes, except for the 50 kDa membrane (Fig. 3). Therefore, it was concluded that the organic matter that is smaller than the pore size had a great potential to foul the membranes irreversibly by pore narrowing.

As mentioned above, the hydraulic backwash on the 50 kDa membrane was able to partially recover the fouling resistance during the permeate water filtration. This is likely due to the possible manufacturing defects on the 50 kDa membrane, as determined from the MWCO measurements (Supplementary Data, Fig. S4). The defects appeared to be minor, since there was always a 90% rejection of molecules larger than 50 kDa. Consequently, small amounts of large particles were present in the permeate water of 50 kDa UF, causing slight cake-layer fouling when filtrating the permeate water. However, no obvious defect was detected on the 0.20 μm, 0.14 μm and 300 kDa ceramic membranes, as evidenced by the pore size distribution and MWCO measurements (Supplementary Data, Figs. S2 & S4).

The assumption that cake layer formation is negligible during permeate water filtration makes it possible to calculate the extent of pore size narrowing on each membrane using the Hagen–Poiseuille equation (Eq. (7)). The pore radius reductions of the 0.20 μm and 0.14 μμm MF membranes were 19.5 nm and 12 nm, respectively, according to the calculation using Eq. (7). These values were also validated using the capillary flow porometry measurements and the measured pore radius reductions were 9.2 ± 1.7 nm and 10.5 ± 1.5 nm, respectively (Table 3). The measured values were of the same order of magnitude as the calculated ones. For the 300 kDa and 50 kDa UF membranes, the pore radius reduction was 2.6 and 1.4 nm, respectively (Eq. (7)). The defects on the 50 kDa membrane might have led to a slight underestimation of its pore radius reduction. The pore radius reduction of the ceramic UF membranes due to the adsorbed organic matter was of the same order of magnitude as molecular length of the humic substances, indicating that a monolayer of humic substances was formed due to the internal fouling. However, in the ceramic MF membranes, the monolayer of internal irreversible fouling was mainly composed of a monolayer of biopolymers or combination of biopolymers and humic substances, according to their pore size reduction.

3.3. Irreversible fouling indices on the membranes with various pore sizes

The hydraulically irreversible fouling indices (HIFI) of the four ceramic membranes were calculated (Eq. (10)) based on the operation data in 12 filtration cycles. A correlation was found between the HIFI values and the membrane pore sizes. The results in Table 4

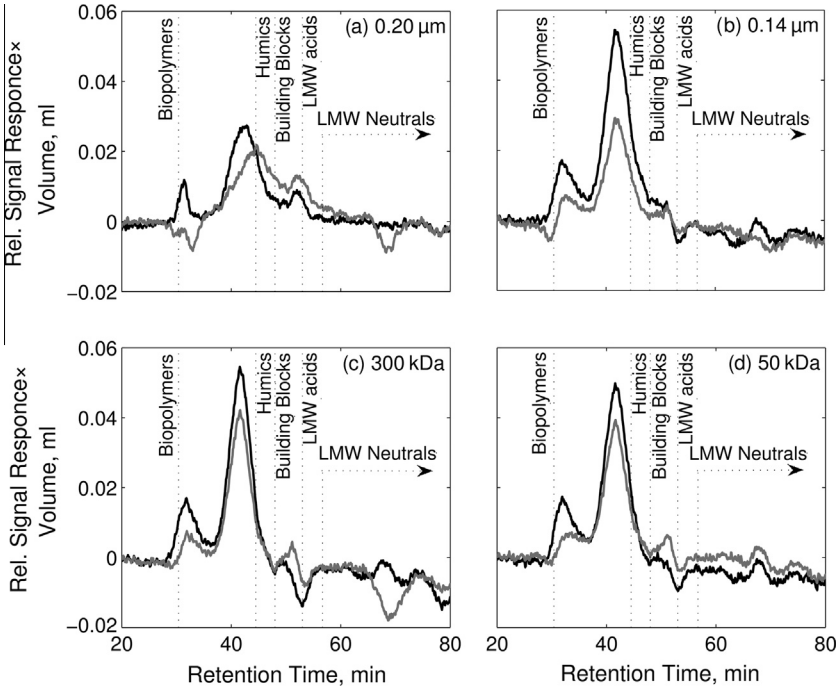

Fig. 2. Organic compositions of the HIF on the (a) 0.20 µm, (b) 0.14 µm, (c) 300 kDa and (d) 50 kDa ceramic membranes. Calculated with mass balance by Eq. (4). (▬ First 3 cycles; ▬ Last 3 cycles).

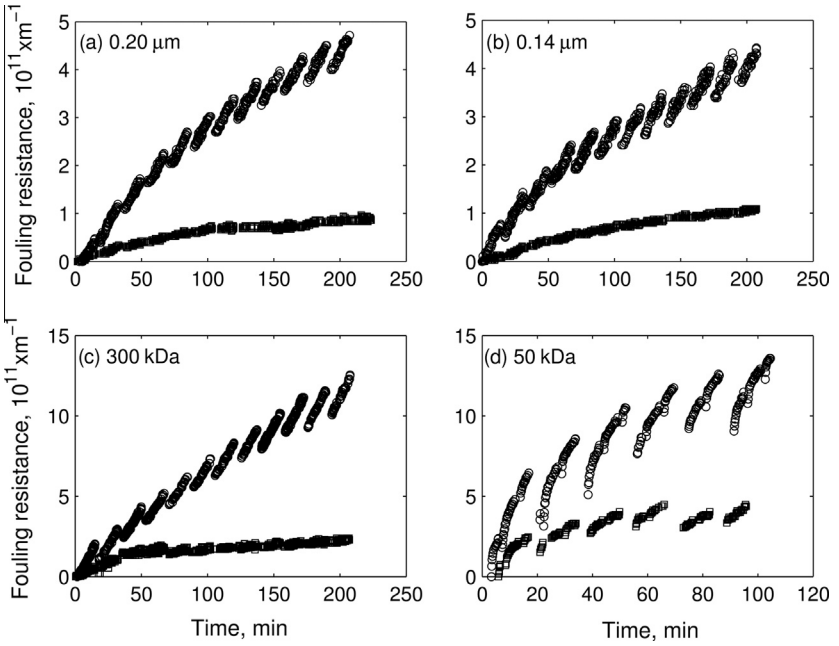

Fig. 3. Fouling resistance during the raw water filtration and permeate water filtration. Both filtration experiments were carried out with 60 L m^{-2} h^{-1} constant flux with forward flush (60 L m^{-2} h^{-1} for 1.5 min), filtrate (for 15 min) and backwash with permeate water (120 L m^{-2} h^{-1} for 3 min). (○ Filtration of surface water; □ Filtration of permeate water).

show that the HIFI values were proportional to the membrane pore size (r^2 = 0.89) when the same feed water was filtrated by these four membranes with different pore sizes. This is probably because less organic matter can enter the membrane pore and form internal fouling, which is mainly hydraulically irreversible fouling.

A different trend was reported by Qu et al. [52] who concluded that a more severe irreversible fouling was found on membranes with a tighter pore size. This is probably because a different feed solution was used with extracellular algae organic matter (AOM) from *M. aeruginosa*. The AOM consists of organic matters of larger molecular weight than 30 kDa [53], while the surface water used in this study contains organic matter of wide molecular weight distribution. Consequently, the difference in feed solutions modifies the fouling mechanisms with regard to internal fouling and cake layer formation. In addition, the hydraulic irreversible fouling is strongly related to the operational conditions of both filtration flux and backwash flux. The different operational conditions in both studies may also lead to diverted fouling behavior.

Table 3
Pore radius of the clean membranes and fouled membranes after hydraulic backwash.

	MF membranes		UF membranes	
	0.20 μm	0.14 μm	300 kDa	50 kDa
r_p of clean membrane (nm)[a]	95.5 ± 1.0	64.5 ± 1.0	30.5[b]	12.5[b]
Measured r_p of fouled membrane (nm)[a]	86.3 ± 0.7	54.0 ± 0.5	–	–
Calculated[c] r_p of fouled membrane (nm)	76.0	52.5	27.9	11.1

[a] Average ± SD from triplicate measurements.
[b] Calculated based on MWCO using Eq. (6).
[c] Calculated from resistance increase during permeate water filtration.

Table 4
Hydraulically irreversible fouling indices (HIFI) of the MF and UF membranes during the operation of 12 cycles.

	UF membranes		MF membranes	
MWCO/Pore size	50 kDa/ 0.025 μm	300 kDa/ 0.061 μm	0.14 μm	0.20 μm
HIFI ($m^2\ L^{-1}$)	0.0026	0.0072	0.0252	0.0297

4. Conclusions

In this work, the hydraulically irreversible fouling on ceramic MF/UF membranes was studied using natural surface water. The composition of hydraulically irreversible foulants and the irreversible fouling index (HIFI) were compared among the tested membranes. The following conclusions were drawn:

(1) With the help of mass balance calculations based on LC-OCD analysis, it was possible to quantitatively illustrate the organic composition of the irreversible foulants. It showed that humic substances and biopolymers in the surface water were the main fractions of the irreversible foulants.
(2) Humic substances and biopolymers resulted in different fouling behaviors on membranes with various pore sizes with regards to internal fouling and cake layer formation. Internal fouling of the ceramic MF membranes mainly resulted from the monolayer adsorption of biopolymers, while the internal fouling on UF membranes was due to the monolayer adsorption of humic substances. Pore narrowing (internal fouling) was found to be a main contributor to hydraulically irreversible fouling.
(3) Membranes with tighter pores showed less irreversible fouling potential (low HIFI values) compared to the ones with opener pores, because less organic matter can enter the membrane pore and form internal fouling, which is mainly irreversible.

List of abbreviations

DOC	dissolved organic carbon
HIFI	hydraulically irreversible fouling index
LC-OCD	liquid chromatography with organic carbon detector
MF	microfiltration
MW	molecular weight
MWCO	molecular weight cut-off
TMP	trans-membrane pressure
UF	ultrafiltration

Acknowledgements

This research work was carried out in the framework of Agentschap NL-international InnoWATOR project "Innovative ceramic ultra and nanofiltration" and Shanghai Science and Technology Project for International Cooperation (Grant No. 12230707602). The authors acknowledge the PhD scholarship awarded to Ran Shang (No. 2009626042) by the China Scholarship Council. Ing. H.A. Teunis and Dr. Ing. Z. Borneman at the University of Twente are acknowledged for the Porometry measurements. We thank the reviewers whose comments were valuable to this manuscript.

Appendix A. Supplementary material

Supplementary data associated with this article can be found, in the online version, at http://dx.doi.org/10.1016/j.seppur.2015.04.039.

References

[1] K. Guerra, J. Pellegrino, Development of a techno-economic model to compare ceramic and polymeric membranes, Sep. Sci. Technol. (Philadelphia) 48 (1) (2013) 51–65.
[2] F.C. Kramer et al., Direct water reclamation from sewage using ceramic tight ultra- and nanofiltration, Sep. Purif. Technol. 147 (2015) 329–336.
[3] G. Galjaard et al., Ceramacspi®-19 demonstration plant ceramic microfiltration at Choa Chu Kang Waterworks, Water Pract. Technol. 7 (4) (2012).
[4] R. Shang, Ceramic Ultra- and Nanofiltration for Municipal Wastewater Reuse, Delft University of Technology, Delft, 2014.
[5] C.M. Urista et al., Critical flux determination in ultrafiltration of wastewater from a food industry by optimization method, Chem. Eng. Commun. 200 (2) (2013) 163–177.
[6] B. Hofs et al., Comparison of ceramic and polymeric membrane permeability and fouling using surface water, Sep. Purif. Technol. 79 (3) (2011) 365–374.
[7] U. Mueller, G. Biwer, G. Baldauf, Ceramic membranes for water treatment, Water Sci. Technol.: Water Supply 10 (6) (2010) 987–994.
[8] X. Zhang, L. Fan, F.A. Roddick, Understanding the fouling of a ceramic microfiltration membrane caused by algal organic matter released from *Microcystis aeruginosa*, J. Membr. Sci. 447 (2013) 362–368.
[9] F. Qu et al., Ultrafiltration membrane fouling by extracellular organic matters (EOM) of *Microcystis aeruginosa* in stationary phase: Influences of interfacial characteristics of foulants and fouling mechanisms, Water Res. 46 (5) (2012) 1490–1500.
[10] W. Yuan, A.L. Zydney, Humic acid fouling during ultrafiltration, Environ. Sci. Technol. 34 (23) (2000) 5043–5050.
[11] C. Jucker, M.M. Clark, Adsorption of aquatic humic substances on hydrophobic ultrafiltration membranes, J. Membr. Sci. 97 (1994) 37–52.
[12] K. Katsoufidou, S.G. Yiantsios, A.J. Karabelas, A study of ultrafiltration membrane fouling by humic acids and flux recovery by backwashing: experiments and modeling, J. Membr. Sci. 266 (1–2) (2005) 40–50.
[13] R. Shang, H.P. Deng, J.Y. Hu, Removal of humic acid by a new type of electrical hollow-fiber microfiltration (E-HFMF), AIP Confer. Proc. 1251 (2009) 97–100.
[14] W. Yuan, A.L. Zydney, Effects of solution environment on humic acid fouling during microfiltration, Desalination 122 (1) (1999) 63–76.
[15] X. Zheng et al., Biopolymer fouling in dead-end ultrafiltration of treated domestic wastewater, Water Res. 44 (18) (2010) 5212–5221.
[16] H. Yamamura, K. Kimura, Y. Watanabe, Mechanism involved in the evolution of physically irreversible fouling in microfiltration and ultrafiltration membranes used for drinking water treatment, Environ. Sci. Technol. 41 (19) (2007) 6789–6794.
[17] K. Kimura et al., Irreversible membrane fouling during ultrafiltration of surface water, Water Res. 38 (14–15) (2004) 3431–3441.
[18] S. Peldszus et al., Reversible and irreversible low-pressure membrane foulants in drinking water treatment: Identification by principal component analysis of fluorescence EEM and mitigation by biofiltration pretreatment, Water Res. 45 (16) (2011) 5161–5170.
[19] M.D. Kennedy et al., Colloidal organic matter fouling of UF membranes: role of NOM composition & size, Desalination 220 (1–3) (2008) 200–213.
[20] J.-Y. Tian et al., Correlations of relevant membrane foulants with UF membrane fouling in different waters, Water Res. 47 (3) (2013) 1218–1228.
[21] K. Kimura, K. Tanaka, Y. Watanabe, Microfiltration of different surface waters with/without coagulation: clear correlations between membrane fouling and hydrophilic biopolymers, Water Res. 49 (2014) 434–443.
[22] X. Zheng, M. Ernst, M. Jekel, Identification and quantification of major organic foulants in treated domestic wastewater affecting filterability in dead-end ultrafiltration, Water Res. 43 (1) (2009) 238–244.
[23] X. Zhang, L. Fan, F.A. Roddick, Feedwater coagulation to mitigate the fouling of a ceramic MF membrane caused by soluble algal organic matter, Sep. Purif. Technol. 133 (2014) 221–226.
[24] K.J. Howe, M.M. Clark, Fouling of microfiltration and ultrafiltration membranes by natural waters, Environ. Sci. Technol. 36 (16) (2002) 3571–3576.
[25] Q. Li, M. Elimelech, Synergistic effects in combined fouling of a loose nanofiltration membrane by colloidal materials and natural organic matter, J. Membr. Sci. 278 (1–2) (2006) 72–82.

[26] J.-Y. Tian et al., Effect of particle size and concentration on the synergistic UF membrane fouling by particles and NOM fractions, J. Membr. Sci. 446 (2013) 1–9.
[27] L. Jin, S.L. Ong, H.Y. Ng, Comparison of fouling characteristics in different pore-sized submerged ceramic membrane bioreactors, Water Res. 44 (20) (2010) 5907–5918.
[28] S. Mafirad, M.R. Mehrnia, M.H. Sarrafzadeh, Effect of membrane characteristics on the performance of membrane bioreactors for oily wastewater treatment, Water Sci. Technol. 64 (5) (2011) 1154–1160.
[29] C.F. Lin et al., Effects of mass retention of dissolved organic matter and membrane pore size on membrane fouling and flux decline, Water Res. 43 (2) (2009) 389–394.
[30] H. Zhu, X. Wen, X. Huang, Characterization of membrane fouling in a microfiltration ceramic membrane system treating secondary effluent, Desalination 284 (2012) 324–331.
[31] A.R. Costa, M.N. De Pinho, Effect of membrane pore size and solution chemistry on the ultrafiltration of humic substances solutions, J. Membr. Sci. 255 (1–2) (2005) 49–56.
[32] S.A. Huber et al., Characterisation of aquatic humic and non-humic matter with size-exclusion chromatography – organic carbon detection – organic nitrogen detection (LC–OCD–OND), Water Res. 45 (2) (2011) 879–885.
[33] E.R. Cornelissen et al., Selection of anionic exchange resins for removal of natural organic matter (NOM) fractions, Water Res. 42 (1–2) (2008) 413–423.
[34] P. Aimar, M. Meireles, V. Sanchez, A contribution to the translation of retention curves into pore size distributions for sieving membranes, J. Membr. Sci. 54 (3) (1990) 321–338.
[35] M.E. Schimpf, M.P. Petteys, Characterization of humic materials by flow field-flow fractionation, Colloids Surf. A: Physicochem. Eng. Aspects 120 (1–3) (1997) 87–100.
[36] J.R. Lead et al., Characterization of norwegian natural organic matter: size, diffusion coefficients, and electrophoretic mobilities, Environ. Int. 25 (2–3) (1999) 245–258.
[37] J. Guo, J. Ma, AFM study on the sorbed NOM and its fractions isolated from River Songhua, Water Res. 40 (10) (2006) 1975–1984.
[38] Huber SA. *DOC-LABOR Dr. Huber: Screening of Organics in Natural and Technical Waters*. [cited 2012; <http://www.doc-labor.de/Sending_samples.html>.
[39] M.H. Friedman, Principles and Models of Biological Transport, Springer, 2008.
[40] R. Shang et al., Tight ceramic UF membrane as RO pre-treatment: the role of electrostatic interactions on phosphate rejection, Water Res. 48 (1) (2014) 498–507.
[41] E.M. Renkin, Filtration, diffusion, and molecular sieving through porous cellulose membranes, J. Gener. Physiol. 38 (2) (1954) 225–243.
[42] C.M. Tam, A.Y. Tremblay, Membrane pore characterization—comparison between single and multicomponent solute probe techniques, J. Membr. Sci. 57 (2–3) (1991) 271–287.
[43] P. Puhlfürß et al., Microporous TiO_2 membranes with a cut off <500 Da, J. Membr. Sci. 174 (1) (2000) 123–133.
[44] M. Mulder (Ed.), Basic Principles of Membrane Technology, Kluwer Academic Publishers, 1991.
[45] L. Palacio et al., Porosity measurements by a gas penetration method and other techniques applied to membrane characterization, Thin Solid Films 348 (1–2) (1999) 22–29.
[46] A.S. Jönsson et al., Influence of the concentration of a low-molecular organic solute on the flux reduction of a polyethersulphone ultrafiltration membrane, J. Membr. Sci. 135 (1) (1997) 117–128.
[47] J. Lindau, A.S. Jönsson, A. Bottino, Flux reduction of ultrafiltration membranes with different cut-off due to adsorption of a low-molecular-weight hydrophobic solute–correlation between flux decline and pore size, J. Membr. Sci. 149 (1) (1998) 11–20.
[48] J.H. Roorda, Filtration Characteristics in Dead-end Ultrafiltration of WWTP-effluent, Delft University of Technology, Delft, 2004.
[49] A.H. Nguyen, J.E. Tobiason, K.J. Howe, Fouling indices for low pressure hollow fiber membrane performance assessment, Water Res. 45 (8) (2011) 2627–2637.
[50] M. Koh, M.M. Clark, K.J. Howe, Filtration of lake natural organic matter: adsorption capacity of a polypropylene microfilter, J. Membr. Sci. 256 (1–2) (2005) 169–175.
[51] K.J. Jim et al., Fouling mechanisms of membranes during protein ultrafiltration, J. Membr. Sci. 68 (1–2) (1992) 79–91.
[52] F. Qu et al., Ultrafiltration membrane fouling caused by extracellular organic matter (EOM) from *Microcystis aeruginosa*: effects of membrane pore size and surface hydrophobicity, J. Membr. Sci. 449 (2014) 58–66.
[53] L. Li et al., Characterization of intracellular & extracellular algae organic matters (AOM) of *Microcystic aeruginosa* and formation of AOM-associated disinfection byproducts and odor & taste compounds, Water Res. 46 (4) (2012) 1233–1240.